

#### **Reviewed Preprint**

Revised by authors after peer review.

About eLife's process

**Reviewed preprint version 2** January 12, 2024 (this version)

**Reviewed preprint version 1** August 10, 2023

Sent for peer review June 7, 2023

**Posted to preprint server** May 10, 2023

#### **Computational and Systems Biology**

## Spatial-temporal orderdisorder transition in angiogenic NOTCH signaling controls cell fate specification

Tae-Yun Kang, Federico Bocci, Qing Nie, José Nelson Onuchic ☑, Andre Levchenko ☑

Department of Biomedical Engineering, Yale University • NSF-Simons Center for Multiscale Cell Fate Research, University of California Irvine • Department of Mathematics, University of California Irvine • Center for Theoretical Biological Physics, Rice University

- https://en.wikipedia.org/wiki/Open\_access
- © Copyright information

#### **Abstract**

Angiogenesis is a morphogenic process resulting in the formation of new blood vessels from pre-existing ones, usually in hypoxic micro-environments. The initial steps of angiogenesis depend on robust differentiation of oligopotent endothelial cells into the Tip and Stalk phenotypic cell fates, controlled by NOTCH-dependent cell-cell communication. The dynamics of spatial patterning of this cell fate specification are only partially understood. Here, by combining a controlled experimental angiogenesis model with mathematical and computational analyses, we find that the regular spatial Tip-Stalk cell patterning can undergo an order-disorder transition at a relatively high input level of a pro-angiogenic factor VEGF. The resulting differentiation is robust but temporally unstable for most cells, with only a subset of presumptive Tip cells leading sprout extensions. We further find that sprouts form in a manner maximizing their mutual distance, consistent with a Turing-like model that may depend on local enrichment and depletion of fibronectin. Together, our data suggest that NOTCH signaling mediates a robust way of cell differentiation enabling but not instructing subsequent steps in angiogenic morphogenesis, which may require additional cues and selforganization mechanisms. This analysis can assist in further understanding of cell plasticity underlying angiogenesis and other complex morphogenic processes.

#### Significance Statement

We investigate the spatial and temporal patterns of Tip/Stalk specification and the ensuing angiogenic sprouting by using a novel controlled micro-engineered experimental model of angiogenesis and a set of mathematical models of the spatially resolved, cell population-level VEGF-NOTCH signaling. Our analysis provides a dynamic view of the initial step of angiogenesis, revealing fluctuations in its onset, and features suggesting transitions between order and disorder in cell organization. These findings suggest how a potentially very restrictive patterning mechanism can become sensitive to a variety of environmental cues. This sensitivity can be crucial for proper vascularization of a damaged organ, and may suggest new ways of analyzing angiogenesis in the context of cancer and other pathologies. This analysis also suggests a framework for understanding of other instances of NOTCH-mediated patterning processes.



#### eLife assessment

The authors used an appropriate micro-engineered experimental model of angiogenesis coupled to mathematical model to study the early steps of the angiogenic sprouting. To this end, the authors developed a **convincing** model to predict how VEGF activates Delta-Notch signaling. The work affords **important** new insight into the complex processes involved in the onset of angiogenesis.

#### Introduction

Angiogenesis, i.e., the formation of new blood vessels from the pre-existing ones, is a striking example of phenotypic plasticity in an adult differentiated endothelium. Pro-angiogenic factors secreted in response to hypoxic conditions, particularly the vascular endothelial growth factor (VEGF), specify differentiation of endothelial cells lining blood vessels into diverse phenotypic states, including the pro-migratory Tip cell phenotype. Tip cells can initiate invasive cell migration into the surrounding extracellular matrix (ECM), leading to sprouting and branching of the nascent vessels(1 2, 2 2). Tip cells are differentiated from Stalk cells, another phenotypic state, through juxtacrine cell-cell interaction between these cell types involving NOTCH1 signaling, triggered and modulated by induction of Dll4 and Jag1 ligands(3 2, 4 2). Stalk cells can therefore form in immediate proximity of Tip cells, particularly, at the leading edge of an extending sprout, if the NOTCH signaling is sufficiently pronounced for the Tip-Stalk differentiation to occur. Proliferation of Stalk cells is as essential as the invasive migration of Tip cells for the emergence, extension and branching of growing sprouts, making the analysis of coordinated Tip and Stalk specification particularly important.

The inputs specifying the cell fate can be potentially contradictory, e.g., with pro-angiogenic factors, such as VEGF, promoting the Tip cell fate, and the NOTCH signaling activated by the neighboring cells promoting the Stalk cell fate and thus suppressing the Tip cell identity in the same cell. These and other signaling inputs can thus be incoherent in terms of cell fate specification and can result in complex dynamic outcomes that are still poorly understood. Further elucidation of these processes thus requires high resolution, quantitative experimental measurements tightly coupled with computational analysis. Since such measurements are still challenging *in vivo*, particularly in mammalian tissues, use of tissue models recapitulating the salient features of the developing vasculature is a key tool in the current analysis of angiogenesis and development of *de novo* vascular beds.

Previously, we and others have developed a set of micro-fabricated experimental angiogenesis models that have had progressively improved biomimetic characteristics(5 2-9 2). These characteristics include spatially and biochemically appropriate cell micro-environments, composed of components of the extracellular matrix and of gradients of growth factors and cytokines around the developing vasculature, which is composed of endothelial cells and pericytes.

We have previously used this approach to map different combinations of VEGF and an inflammatory cytokine, TNF, onto pro- and anti-angiogenic outcomes, modeling frequently encountered angiogenesis conditions(7년). This analysis provided evidence that 'mini-sprouts' — one-cell structures protruding from the parental blood vessel into the surrounding matrix — were comprised of Tip cells. However, it was not clear whether all such 'mini-sprouts' would ultimately develop into more mature multi-cellular sprouts with defined lumens and the potential to form



new blood vessels. Furthermore, although our analysis was successful in explaining the fraction of Tip cells formed under different conditions, it was not clear how to account for the spatial aspects of the Tip cell and mature sprout specification, such as their mutual separation and density.

We address these challenges here by extending our analysis to a higher temporal and spatial resolution, both in experimental and mathematical models of angiogenic sprouting. Surprisingly, we found that the formation of mini-sprouts was a highly dynamic process, in which they could either retract after extension or form full-fledged sprouts. Furthermore, the experimentally determined spatial positioning of mini-sprouts was well explained by the predicted locations of the Tip cells in the mathematical model but the model could not account for which of the mini-sprouts would become fully formed sprouts. Further analysis revealed that the stable sprout formation from mini-sprouts can be enabled by the local fluctuations of the density of fibronectin, a key pro-angiogenic ECM component, leading to sparse patterns where sprouts tend to maximally distance themselves from other fully formed sprouts. These results reveal some of the key mechanisms that may define the density of the angiogenically formed vascular beds under diverse conditions.

#### **Results**

# Dynamic angiogenesis can be explored in a 3D biomimetic experimental setup

To investigate the properties of angiogenic patterning and cell fate specification, we used an experimental model previously employed to assess the crosStalk between pro-angiogenic and proinflammatory stimuli(7 \(^2\)). In this experimental setup, angiogenesis occurs from a 3D parental engineered endothelial vessel embedded in the collagen matrix and exposed to exogenously supplied VEGF and other pro-angiogenic factors (Fig. 1A-B 🖒). In agreement with prior observations, we found that this setup resulted in formation of both one-cell extensions into the matrix (mini-sprouts) and full-fledged multi-cellular sprouts containing detectable lumens and pronounced leading Tip cells (**Fig. 1C** ○ ). Sprouts displayed a variety of growth stages, including the very early ones, composed of one lumenized cell or pairs of connected cells, also forming a lumen (Table 1 22). Although mini-sprouts formed throughout the observation area of the vessel, sprouts developed within specific zones, while other zones remained devoid of detectable sprout formation over the course of the study (Figs. 1D-F .). These observations suggested that cell fate specification and sprout formation are dynamic processes that may display diverse local outcomes. We therefore set out to characterize these processes in the context of an accessible and well defined analysis tool that can allow to contrast experimental findings with mathematical models of angiogenic patterning, particularly those based on the commonly assumed NOTCH receptor mediated cell-cell interactions (Fig. 1G 🖒).

# Mathematical model of VEGF/NOTCH signaling predicts spatially resolved Tip-Stalk patterns

To set the framework for the analysis of cell fate determination, we extended our previously developed and experimentally validated mathematical model of Tip-Stalk fate differentiation between two cells(10 ) to a multicellular hexagonal lattice in two-dimensions. In the new model, we replicated within each cell the signaling network incorporating the NOTCH and VEGF pathways (Fig. 2A ). Prior analysis of this model on the level of two adjacent cells predicted the emergence of bistability between a (high NOTCH, low Delta) Stalk phenotype and a (low NOTCH, high Delta) Tip phenotype(10 ). This result is consistent with the overall expectation of the differentiation effect of Delta-NOTCH signaling, which in 2D is further expected to generate 'salt-and-pepper 'patterns, with a single Tip cell surrounded by 6 Stalk cells (11 ), yielding the overall fraction of

# Early Stage I Multi-cells face each other and form a lumen. Early Stage II Luminization occurs within a migrating cell. Matured Stage A leading cell is followed by multiple cells with a lumen. Mini-sprout Cells change polarity and migrate but luminization is not observed.

Table 1.

Phenotypic categorization of sprout and mini-sprout.

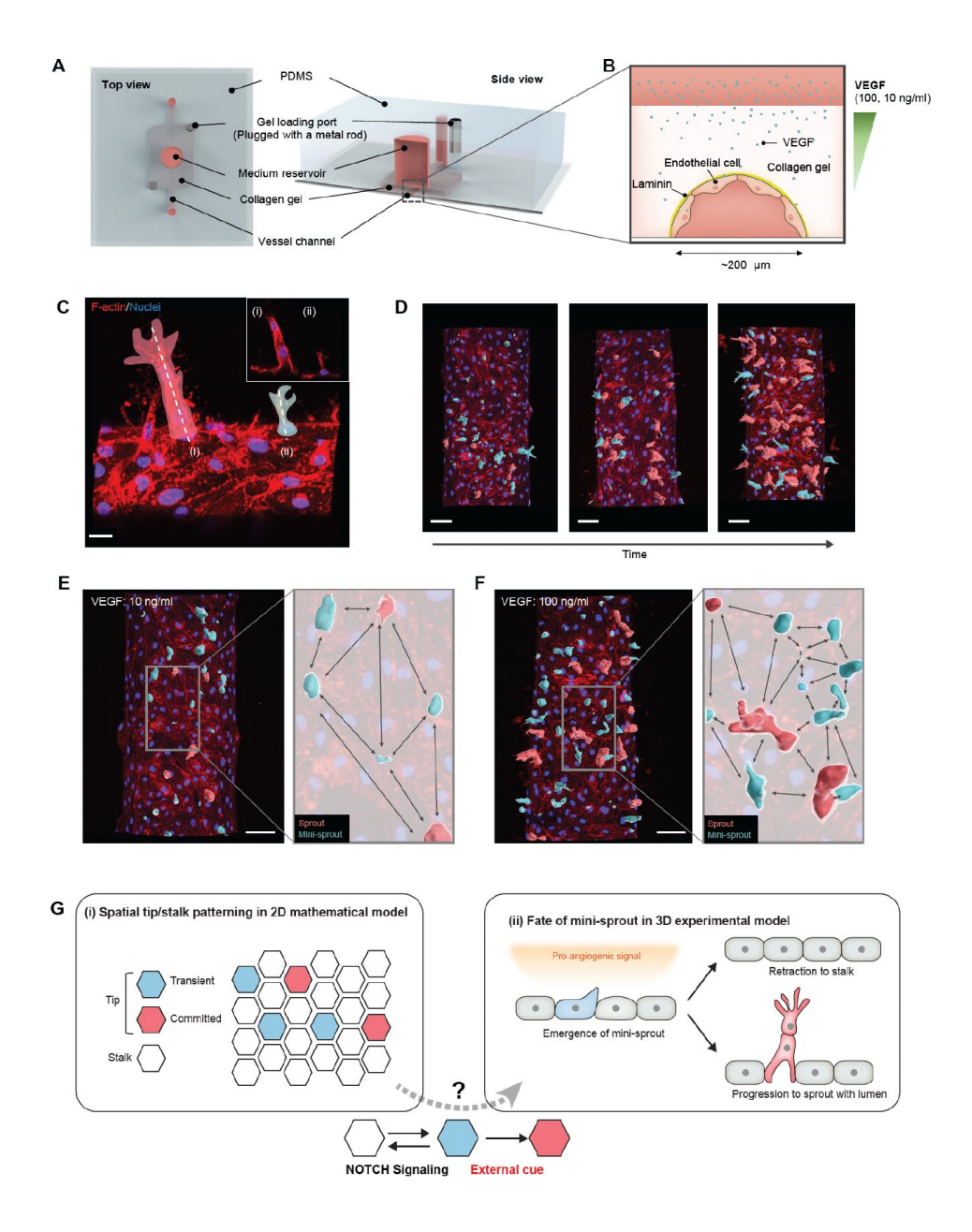


Figure 1.

## Analysis of temporal and spatial regulation of angiogenic fate specification in a 3D biomimetic experimental setup.

(A) 3D vessel model for inducing angiogenesis in response to a gradient of VEGF. (B) Cross-section of a vessel embedded in collagen type I within the device; VEGF is added to the medium reservoir above the vessel to generate a VEGF gradient. (C) Angiogenesis leads to the formation of new sprout-related structures from the parental vessel that have two distinct morphologies: (i) full-fledged multi-cellular sprouts containing detectable lumens, (ii) mini-sprouts in the form of single cell extension into the matrix. Scale bars:  $20~\mu m$ . (D) Temporally resolved observation of dynamic formation of sprouts and mini-sprouts populations during angiogenesis. As depicted in (C), sprouts are pseudo-labeled with red color and mini-sprouts in blue color. Scale bars:  $50~\mu m$ . Dependence of the spatial distribution of sprouts and mini-sprouts on the VEGF concentration: (E) 10~ng/ml and (F) 100~ng/ml. Scale bars:  $50~\mu m$ . Images are 3D reconstructions of confocal z-stacks, showing nuclear (DAPI) and cytoskeleton (Phalloidin). (G) Schematic overview of Tip-Stalk patterning: (i) Spatial Tip-Stalk patterning due to juxtacrine NOTCH signaling that might lead to fixed persistent and transient cell fate specification. (ii) Fates of mini-sprouts in experiments: both retraction (thus conversion from the phenotypically Tip to as Stalk phenotype) and stabilization and growth to a fully defined sprout are observed.



Tip cells in this arrangement of 25%. However, this simple bistability and spatial patterning picture can be altered by signaling inputs that potentially conflict with those involved in Delta-NOTCH signaling (Fig.1G). For example, the VEGF pro-angiogenic factor promoting the Tip cell fate, can conflict with the NOTCH signaling activated by the neighboring cells that instead promotes the Stalk cell fate while suppressing the Tip cell identity. This might result in disordered patterns with adjacent Tip cells that deviate from the archetypical salt-and-pepper configuration. To explore the properties of this disordering effect, we ran simulations, in which the VEGF-NOTCH signaling occurred in all individual cells within a hexagonal array of the model multi-cellular endothelium, starting from randomized initial conditions (Fig. 2A 🖒). The fully equilibrated patterns were then analyzed for distributions of the simulated Delta and NOTCH expression across the cells. We found for a wide range of VEGF inputs that the distributions of Delta and NOTCH displayed largely bimodal distributions, and the levels of the average Delta expression increased with the increasing input (Fig. 2B-C , supplementary Fig. 1A-B) due to positive effect of the activated VEGF receptor on Delta (see again the circuit in Fig. 2A C). Nevertheless, the clear overall bimodality allowed us to consistently classify cells into the Delta-high ('Tip') and Delta-low ('Stalk') cell states and examine the spatial distribution of these cellular sub-types (see Method section: Definition of Tip cells in the model).

The spatial Tip-Stalk cell distribution patterns revealed a complex dependency on the VEGF input. At relatively low VEGF levels, the patterns were mostly ordered, with small deviations from the expected 'salt and paper 'geometry with a 25%-75% ratio of Tip-Stalk (Fig. 2D 🖒). However, as the VEGF input increased, the fraction of Tips grew and the patterns became sharply more disordered over a relatively narrow range of magnitude of the VEGF input, which could be identified as a highly sensitive area separating more 'ordered-like' and 'disordered-like' patterns. Finally, increasing VEGF stimuli beyond the highly sensitive area further increased the disorder of the patterns, but with a lower VEGF sensitivity, over several more orders of magnitude of VEGF inputs (Fig. 2D-E 🗹 and supplementary Fig. 1A-B). Spatial patterns in the disordered phase at high VEGF input levels were characterized by much higher fractions of Tip cells that were frequently in contact with each other as quantified by a "disorder index" (supplementary Fig. 1C-D). This transition was reminiscent of the order-disorder transition commonly observed and studied in the change of the order of atoms in various substances as a function of temperature, and in other chemical systems (12 2, 13 2). As expected for these types of transitions, increasing or decreasing the order-stabilizing Delta-NOTCH cell-cell signaling, resulted in the corresponding shifts of the ranges of VEGF inputs, over which the sharp order-disorder transition occurred. For example, a small increment or decrease in the cellular production of the Delta ligand shifted the orderdisorder transition to either lower or higher VEGF inputs (Fig. 2F ...). As the broad sweep of the VEGF inputs simulated in the mathematical model is likely beyond the range of receptor sensitivity for the experimental VEGF signaling, we contrasted the predicted fractions of Tip cells with the previously made observations in the 3D experimental angiogenesis model shown in Fig. 1 ☑. We found that, for the VEGF = 10 ng/ml, the experimentally determined fraction of the Tip cells was  $0.20 \pm 0.08$  (mean  $\pm$  SD), i.e., encompassing the fraction of 0.25 expected for the completely ordered, 'salt-and-pepper 'Tip cell distribution pattern. However, for VEGF = 100 ng/ml the experimentally observed Tip cell fraction was 0.32 ± 0.01 (mean ± SD), which corresponded to the disordered state predicted by the model under higher VEGF inputs. We therefore concluded that the transition between order and disorder can occur in the 10-100 ng/ml range of VEGF concentration, allowing us to investigate the properties of the disordered state and its relationship to the spatial frequency of sprout formation. Based on the Tip/Stalk cell ratio, we calibrated the model's parameters so that a VEGF input of 100 ng/ml matched the experimentally observed Tip/Stalk fractions at the same experimental VEGF input (see Methods section: Mathematical model of VEGF/NOTCH signaling).

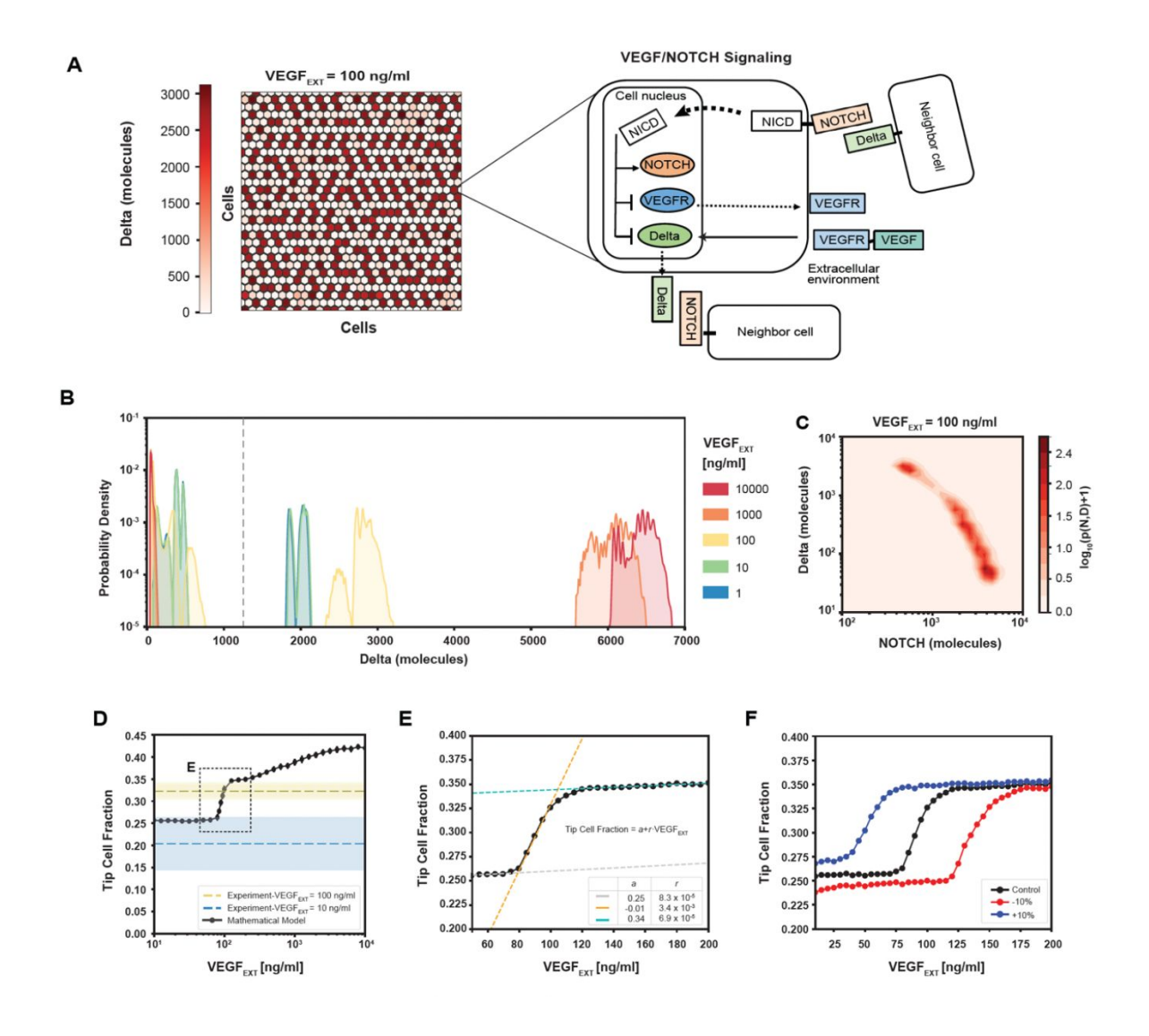


Figure 2.

#### Robust differentiation and order-disorder transition are suggested by mathematical and experimental analyses.

(A) Right: An example of a pattern after full equilibration on a 30x30 hexagonal lattice. Color scale highlights the intracellular levels of Delta. Left: The circuit schematic highlights the components of the intracellular NOTCH-VEGF signaling network. (B) Distribution of intracellular Delta levels in the two-dimensional lattice for increasing levels of external VEGF stimuli. (C) Pseudopotential landscape showing the distribution of intracellular levels of NOTCH and Delta for VEGF<sub>EXT</sub>=100 ng/ml. (D) Fraction of Tip cells as a function of external VEGF stimulus (black curve). Blue and yellow lines and shading depict experimental fractions of Tip cells for VEGF<sub>EXT</sub>=10 ng/ml and VEGF<sub>EXT</sub>=100 ng/ml, respectively. (E) Detail of Tip cell fraction transition zone (corresponding to box in panel D). Legend depicts the coefficients of the linear fits. (F) Shift of the VEGF<sub>EXT</sub> transition threshold upon variation of the NOTCH-Delta binding rate constant. For panels B-F, results are averaged over 50 independent simulations starting from randomized initial conditions for each VEGF<sub>EXT</sub> level (See Methods section: Simulation details).



# Precise quantification of Tip cell spatial arrangement suggests disordered patterning in the engineered angiogenesis model

To enable the comparison between the modeling predictions and experimental observations, we first quantified the spatial patterning characteristics of the inferred positions of the Tip cells in the experimental angiogenesis model. As in our prior analysis using this experimental approach (7 ₺), we identified Tip cells based on their key *phenotypic* characteristic — invasive migration into the surrounding collagen matrix. As suggested above, Tip cells can either be present in the form of 'mini-sprouts' or be at the Tips of sprouts containing recognizable lumens (see Fig. 3A 🗹 and **Table 1** of for examples of this classification). Since formation of both mini-sprouts and lumenized sprouts involved emergence of Tip cells specified in endothelial cell monolayer lining the parental vessel, we constructed a two-dimensional map of the experimentally inferred spatial positions of Tip cells at the location of all mini-sprouts and sprouts (Figs. 3A & B C). This mapping (see Methods section: Quantification of Tip-Tip cell distance in experiments) assumed that the Stalk cells found in the extending sprouts emerge through cell proliferation, rather by Stalk cell migration from the parental vessel. Experimentally, we used nuclear staining to identify non-Tip cells. Since the results above suggested that the cell fates and their patterns in our experimental setup were consistent with the ordered or somewhat disordered 'salt-and-paper 'patterns, we further assumed that all the non-Tip cells adopted the Stalk fates (in the sense of Delta-low, NOTCH-high status, alternative to the Tip cell fate). The resulting map of experimentally specified Tip and Stalk cell locations was then used to calculate the shortest distances between Tip cells, measured in 'cell hops', i.e., the minimal number of intermediate cells between randomly chosen pairs of Tip cells (Fig. 3B 🖒). These distances included Stalk cells exclusively, and no intermediate Tip cells. If two or more Tip cells were at equal distance from a given other Tip cell, their distance ranking was assigned randomly (e.g., two Tip cells at the equal minimal distance to a given Tip cell, would be randomly assigned the ranking of the closest and second closest Tip cell). We then analyzed these data for the VEGF<sub>FXT</sub>= 100 ng/ml experimental input which resulted in the most robust sprouting, comparing the results with the predictions of our mathematical model for the same input level that, when averaging over mulTiple simulations, matched the experimentally measured fraction of Tip cells. Finally, we quantified the shortest paths separating Tip cells in the equilibrated patterns (Fig. 3C 🗗 and Methods section: Quantification of Tip-Tip cell distance in modeling).

The processing of experimental data described above permitted a direct comparison of modeling predictions and experimental defined Tip cells locations, First, we examined the average distances from the Tip cells to the closest, second closest, etc. neighboring Tip cells. We found that this distance distributions closely agreed with the modeling predictions, particularly for the distances up to the 4th closest neighbor, differing substantially from the predictions for the ordered 'saltand-pepper 'patterns (Fig. 3D 🖒). A key finding was that, in agreement with the expectation from the disordered pattern model, there were frequent cases of direct contact between two Tip cells, making the average distance to the closest Tip cell around 0.5 cells in the model. In contrast, two Tip cells were always separated by at least one Stalk cell in "traditional" 'salt- and-pepper 'models. As a baseline comparison, the mathematical model with a 100-fold reduction of VEGF stimulus (1 ng/ml) exhibited a Tip-Tip distance statistics more closely comparable with the 'salt-and-pepper' models. Further analysis of the experimental distributions of Tip cell distances revealed that Tip cells were adjacent to at least 1 other Tip cell with 80% chance, and with at least 2 other Tip cells with 40% chance, and with at least 3 other Tip cells with 20% chance (Fig. 3E ). These Tip cell distance distributions were again in agreement with the modeling results. Taken together these findings provided strong evidence for the predicted partially disordered pattern of Tip cell specification. In our experiments, the observed cell-cell contact area varied, spanning from almost corner-to-corner contact up to approximately 50µm. Previous studies(14 ♂, 15 ♂) have clearly demonstrated the influence of the cell-cell contact area on NOTCH Signaling, but the values get nosy in the middle range, particularly when excluding extremely low cell-cell contact areas. Reflecting these findings, we excluded the corner contacts, which might correspond to extremely

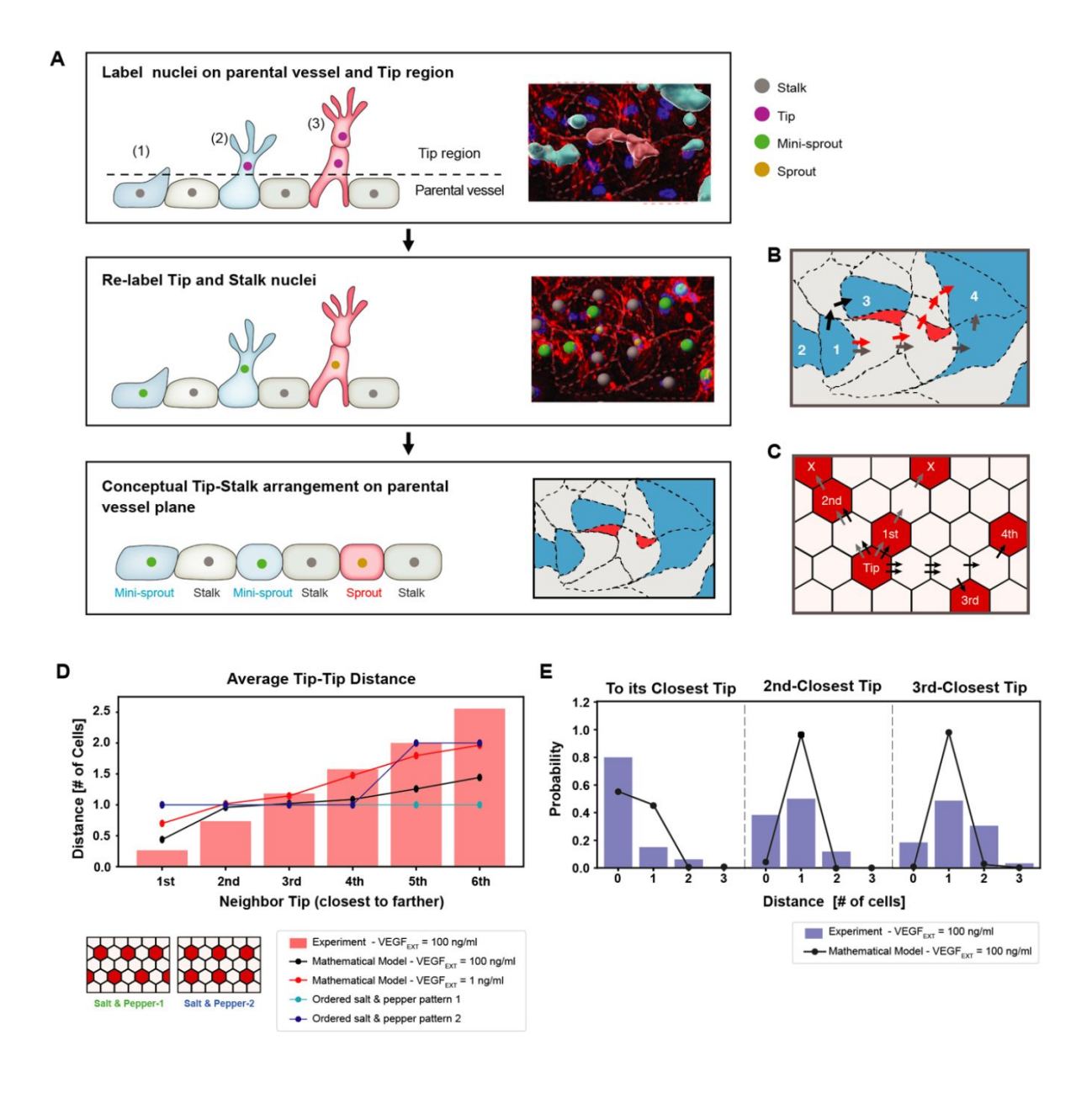


Figure 3.

## Experimentally measured spatial distribution of Tip cells defined as constituting minisprouts and leading sprouts is consistent with the mathematical model predictions.

(A) Analysis pipeline to infer the 2D Tip-Stalk arrangements from 3D experimental images: experimental labeling of the nuclei of sprout/mini-sprout cells (above the plane of the parental vessel) and of the Stalk cells (below the plane of the parental vessel) is used to 'compress' the cells in each sprout or mini-sprout into a single Tip cell. Tip-Tip distance is defined as the number of cells measured in 'cell hops', i.e., the minimal number of intermediate cells between randomly chosen pairs of Tip cells from experiments (B) (the example is identical to the inset at the bottom of (A)) and 2D Tip-Stalk patterns from mathematical modeling (C). Black arrows indicate minimal and valid cell hops between Tips, whereas grey arrows indicate minimal but invalid cell hops (passing through other Tip cells); red arrows indicate the non-minimal cell hops which does not count in the Tip-Tip distance quantification. (D) Tip cell distance distribution from any given Tip cell. Red bars depict experimental measurement for VEGF<sub>EXT</sub>=100 ng/ml and black line depicts the model's prediction for VEGF<sub>EXT</sub>=100 ng/ml. For reference, dashed lines indicate the expected Tip-Tip distance distribution of "perfect" salt-and-pepper patterns shown in the inserts. (E) Detailed distance distribution for the closest Tip (left), second closest Tip (middle), and third closest Tip (right).



low cell-cell contact areas, from the Tip-Tip distance measurements as depicted in **Fig. 3B** . We also made an assumption that variations in cell-cell contact size within tens of microns correlate weakly with the strength of NOTCH signaling. This assumption did not impede our effort to compare the overall trends with results from modeling using hexagonal cells, as shown in **Figs 3 D&E** .

#### Dynamic tracking of angiogenic cell fate specification

The integrative, computational and experimental, analysis presented above suggested that the spatial Tip cell distribution can be well explained by the model of a partially disordered 'salt-andpepper' mechanism. However, it is not clear whether all such Tip cells would spearhead the formation of a new sprout, or retract back to an alternative (Stalk) cell fate. We addressed this question by dynamically tracking the fates of mini-sprouts to examine whether this state is an intermediate step towards the sprout formation. Specifically, we imaged the progress of sprouting in the same areas of a live parental vessel at different time points of 1 hour, 3 hours, 7 hours and 28 hours of incubation in 100 ng/ml of VEGF (Fig. 4A-H 🖸 ). We found that all sprouts formed either directly from Stalks or from mini-sprouts, suggesting a non-observed transition from Stalk to mini-sprout due to observational timeframe limitations. Strikingly, however, not all minisprouts persisted and initiated sprout formation. Instead, many mini-sprouts retracted and new mini-sprouts formed during the time-course of the analysis. We then tracked a group of 118 cells that adopted the mini-sprout phenotype at least once over a period of 28 hours after VEGF exposure. Their state change dynamics was visualized using the Sankey diagram (Fig. 41 2). The initial state of any sprouts or mini-sprouts was classified as the Stalk cell to reflect the hypothesized 'salt-and-pepper 'patterning structure, entirely consisting of either Tip or Stalk cells. When a mini-sprout retracted, it was newly marked as a Stalk cell. By the final time point of 28 hours of VEGF exposure, 45.8% of the cells that displayed the mini-sprout phenotype at least once during the experiment retracted back to the Stalk state, illustrating the highly dynamic phenotype of mini-sprout extensions and retractions. Of the remaining cells, 41.5% and 12.7% were classified to be either in the mini-sprout or sprout-leading Tip cell states, respectively. Although sprout formation continued throughout the experiment, the rate of conversion of mini-sprouts to fullfledged sprouts gradually decreased over time, with 13.6%, 2.9%, and 7.5 % of mini-sprouts becoming sprout-leading Tip cells in the time ranges of 1-3, 3-7 and 7-28 hours. respectively (Fig. **4K-M** □ In most cases (86.7%), sprouts emerged from *newly formed* mini-sprouts (i.e., the cells that were Stalk cells and then mini-sprouts in the preceding two time points), suggesting that minisprouts represent transient states rapidly converting to either the fully committed sprout state or to the Stalk state (Fig. 4 0 ). These observations raised the question of what might define the commitment of a mini-sprout to the sprout differentiation. We next addressed this question by analyzing the spatial distribution of fully formed sprouts over the observed area of the parental vessel.

# Random uniform model accounts for spatial distribution of extending sprouts

While the NOTCH/VEGF mathematical model could quantitatively resolve Tip-Stalk spatial patterns, it did not capture the rate of cell fate switching or explained the commitment of Tip cells to lead the formation of a mature sprout. To identify the underlying principles of sprout initiation, we thus integrated the multicell model with several alternative phenomenological hypotheses (summarized in Fig. 5A-D ). We then tested these hypotheses against the measured distributions of distances between sprouts and, in particular, the observation that sprouts were always separated by at least one non-sprout cell (blue bars in Fig. 5E ). In these tests, we ensured that the results were normalized to the overall density of sprouts observed experimentally (see Method section: Phenomenological models of Sprout selection). The first straightforward hypothesis was that mini-sprouts commit to the sprout phenotype independently of the location of other forming sprouts, constituting the "cell-autonomous sprout selection" model (Fig. 5A-B ). In this case,

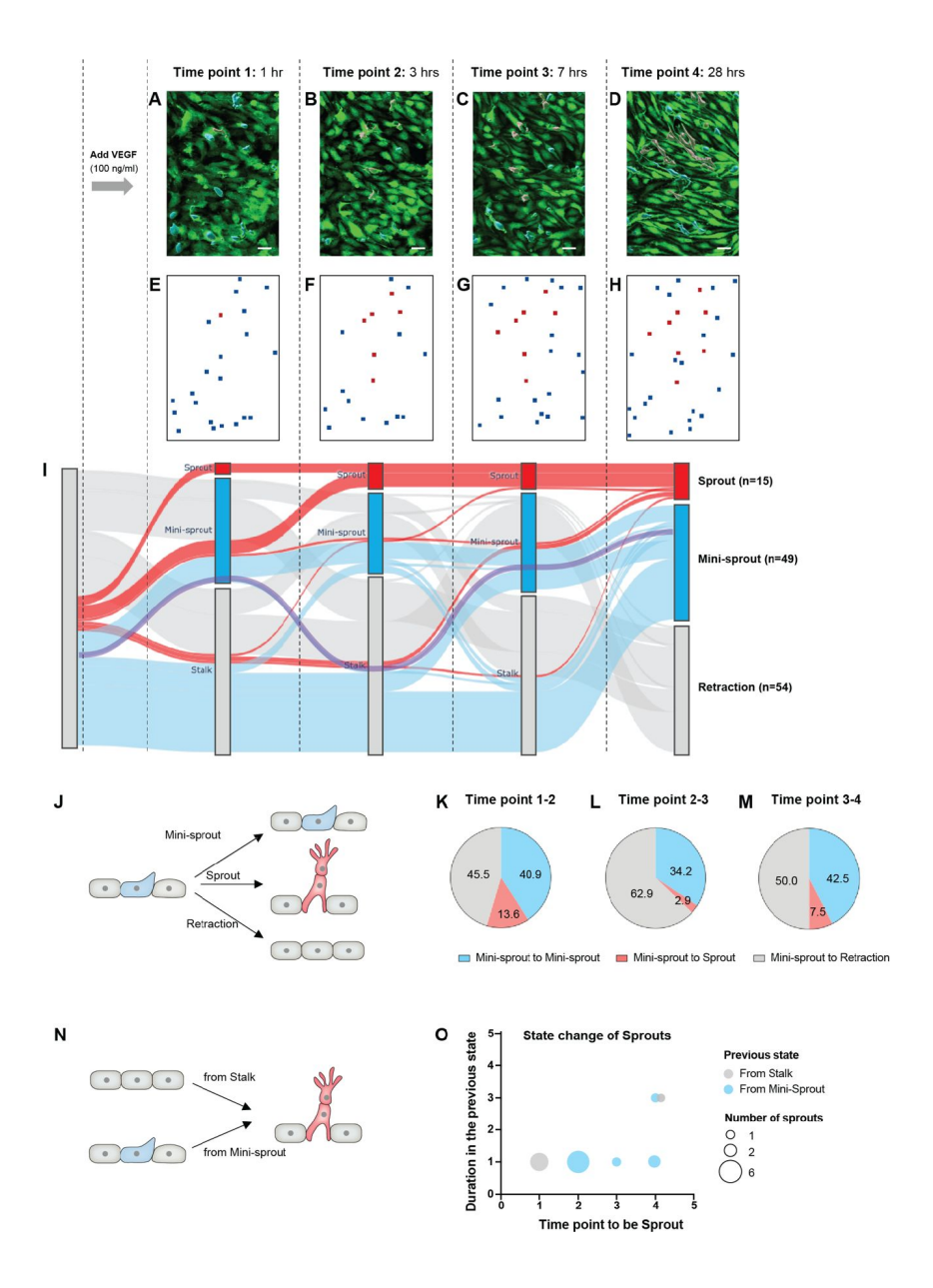


Figure 4.

## The dynamics of mini-sprout and sprout formation suggest frequent mini-sprout retractions, since only a subset of mini-sprouts becoming fully formed sprouts.

GFP-expressing endothelium in the 3D vessel setup captured 1 hour (A), 3 hours (B), 7 hours (C), and 28 hours (D) after 100 ng/ml of VEGF treatment. Sprouts and mini-sprouts are identified by red and blue surface entities, respectively. Square marks representing the positions of sprouts (red) and mini-sprouts (blue) in the original images at each time point (E-H). (I) Sankey diagram demonstrating the dynamic state change of sprouts with red lines and mini-sprouts with blue lines throughout the time points. And grey lines represent mini-sprouts which ended up being retracted at the last observation, time point 4. A purple line shows an example of the state change from a Stalk (initially non-invading endothelial cell) to mini-sprout, retraction, mini-sprout, and mini-sprout at each time point. Only cells that that became mini-sprout at least once during the experiment are shown. (J) Different types of observed transitions between consecutive time points when starting from the mini-sprout state: maintain the mini-sprout state, become a sprout, or retract to the Stalk state. The ratio of states switched from mini-sprouts in the previous time point 1 (K), time point 2 (L), and time point 3 (M). (N) The two observed pathways to sprout formation between consecutive time points: direct Stalk to sprout or mini-sprout to sprout transition. Once a newly formed vessel becomes a sprout, it is permanently committed. (O) Duration of staying as a mini-sprout or a Stalk in the previous state before being committed to a sprout.



however, the corresponding model predicted mulTiple contacts between sprouts (black line in **Fig. 5E** ), in sharp contrast with the experimental observation. The observation that most sprouts are in contact with at least another Tip (Supplementary figure 2A), but never in contact with another sprout, suggested a control mechanism where sprout selection inhibits nearby Tip cells from committing to the same fate. This led to two additional alternative hypotheses. In "repulsion between sprouts" model, it was assumed that sprouts cannot be in contact; therefore, Tip cells cannot commit to the sprout phenotype if already in contact with a sprout (**Fig. 5C** ). In the "random uniform" model, it was assumed that sprouts are selected randomly, but maximizing their overall spread in the lattice (**Fig. 5D**; see Method section: Phenomenological models of Sprout selection). While both models correctly predicted sprouts to never be in contact, the "random uniform" model better described the cases where adjacent sprouts are separated by two or more cells (**Fig. 5E**).

To test these mechanisms more rigorously, we computed the average distance (in cell numbers) between pairs of closest sprouts while also varying the number of sprouts allowed in the lattice (supplementary figure 2B-D), thus generating a curve of the typical sprout-sprout distancing as a function of sprout density in the lattice (**Fig. 5F** ). The "random uniform" model predictions agreed very closely with the experimentally observed combination of sprout fraction and sprout-sprout distance, whereas the other two models greatly underestimated the distances between sprouts (**Fig. 5F** ). Furthermore, while all models overestimated the fraction of the adjacent sprouts that are one cell away from the current sprout and underestimated the fractions of sprouts at greater distances, the deviation of the "random uniform" model predictions for this inter-sprout distribution was the lowest of all the models, again supporting the 'random uniform' model as the more likely to account for sprout selection (**Fig. 5F**).

#### Fibronectin distribution may mediate sprout induction

Random distribution maximizing the distance between sprouts is similar to allelopathy models, accounting to spatial dispersion of species maximizing distance between them. In these models, the key postulated mechanism is inhibition of growth of individuals of the same species through a mutual suppression mechanism(16 -18 ). Another analogous set of mechanisms are embedded within the concept of the Turing pattern formation, the key to which is diffusible negative feedback regulator setting spatial distribution of morphogenic features (19 , 20 ). A variant of such mechanisms is a model postulating depletion of some ingredient that is key to the local growth, by its active redistribution towards the growing pattern features and depletion from the zones between them, rather than active mutual inhibition of the pattern forming units.

Given these prior models, we hypothesized that a similar mechanism may account for the dispersion patterns of sprouts. We focused on the extracellular matrix as a possible medium accounting for the positive and negative pattern-setting interactions. Indeed recently, it has been observed that collagen can be re-organized by the growing sprouts, so that it is concentrated around the extending sprouts and depleted elsewhere(21 2-23 2). We explored whether a similar distribution is also be observed for fibronectin, an ECM component that is critical for the formation of lumenized sprouts (24 2-27 2). Fibronectin expression levels in the vicinity of individual cells comprising the parental vessel and the emerging sprouts was experimentally assessed by immunostaining, with simultaneous cell identification using induced cytoplasmic GFP expression and nuclear staining, followed by 3D reconstruction (Figs. 6A-H 2). Untreated quiescent cells (No treatment) and mini-sprouts showed similar levels of fibronectin expression (Fig. 6H 2). Interestingly, the fibronectin expression was highly enriched at the base but not the Tip areas of the extending sprouts, suggesting that it may be a key determinant of sprout induction but not extension (Figs. 6B,C, &H 2).

We also examine the regional variation of fibronectin expression in larger areas, which was less variable and potentially more relevant to sprout extension. In particular, we accessed the ratio of cells having fibronectin levels higher than a threshold in groups of 7 cells around sprouts and

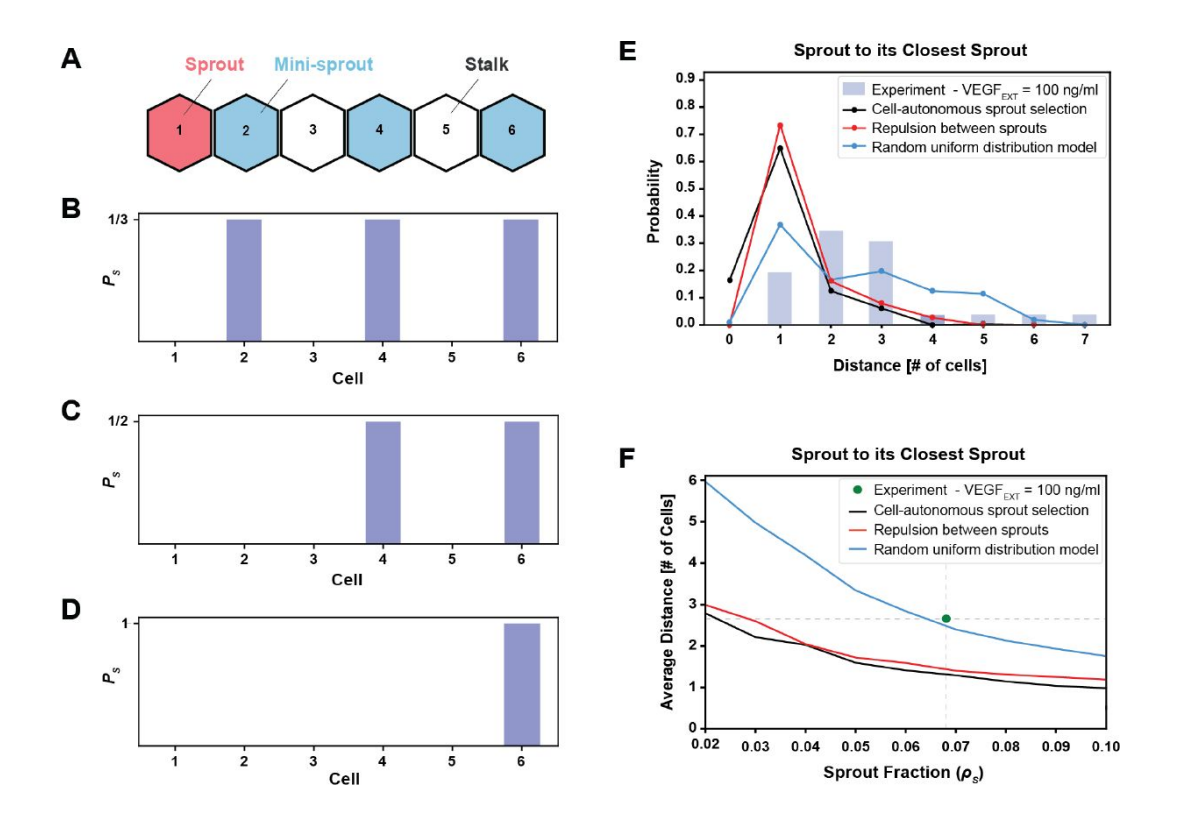


Figure 5.

## The phenomenological model favoring maximal sprout-sprout distances for a given number of sprouts (random uniform distribution) is most consistent with the experimental observations.

(A) An example of 1-dimenstional Tip cell distribution, including a sprout and mini-sprouts, and Stalks pattern. (B) Sprout selection probability ( $P_S$ ) for the cell-autonomous model if a new sprout was added to the pattern of (A). Stalk cells cannot become sprouts, and existing mini-sprouts share the same selection probability. (C) Sprout selection probability ( $P_S$ ) for the sprout repulsion model. The leftmost mini-sprout cannot be selected because it is already in contact with an existing sprout, while the remaining two mini-sprouts share the same selection probability. (D) Sprout selection probability ( $P_S$ ) for the random uniform distribution model. The rightmost mini-sprout maximizes the distance to the existing sprout and is therefore the only viable selection. (E) Sprout distance distribution to its closest sprout neighbor. Blue bars indicate experimental results for VEGF<sub>EXT</sub>=100 ng/ml while black, red and blue lines depict the three different models of sprout selection (cell-autonomous, repulsion between sprouts, and random uniform distribution, respectively). (F) Average distance between a sprout and its closest sprout neighbor in the model as a function of sprout cell fraction in the lattice for the three proposed models of sprout selection. The green dot highlights the experimental sprout fraction and distance at VEGF<sub>EXT</sub>=100 ng/ml.

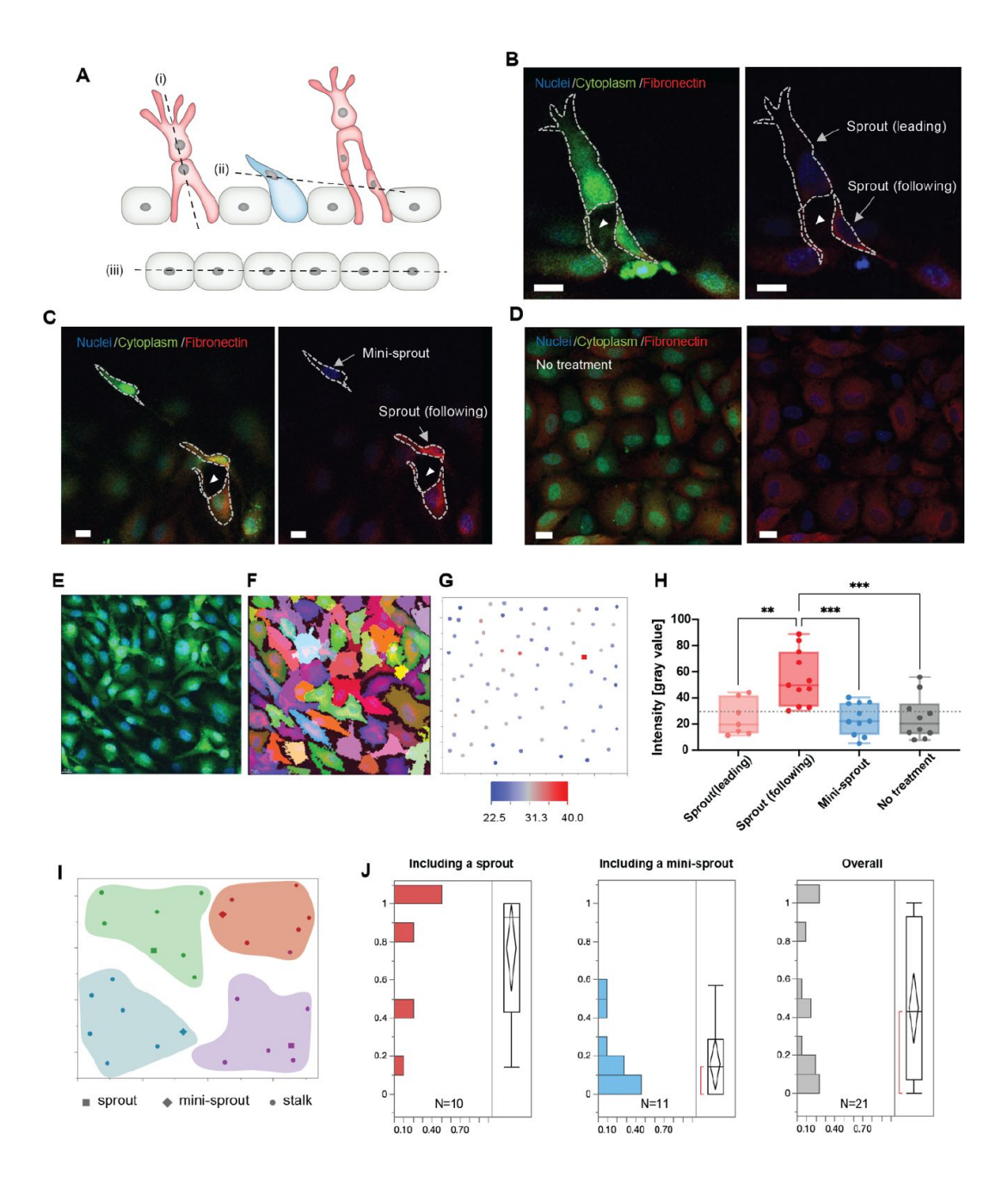


Figure 6.

### Fibronectin distribution on parental and newly formed vessels reveals preferred distribution at the bases of sprouts.

(A) A schematic describing cross-sectional planes for subsequent confocal images: (i) for (B), (ii) for (C), and (iii) for (D). (B) Localization of fibronectin expression to a following cell than in a leading cell in a sprout. (C) Higher fibronectin expression in a sprout (a 'following' cell at the base of the sprout) than at a mini-sprout. (D) Intrinsic heterogeneity of fibronectin expression on quiescent endothelium displaying no mini-sprout or sprout formation. Images are 3D reconstructions of confocal z-stacks. Scale bars: 15  $\mu$ m. Cells on the parental vessel were identified by GFP expression in the cytoplasm (E), then segmented (F). (G) Fibronectin intensity of each cell on the parental vessel is marked as a dot at the corresponding x and y positions of the cell centroids. Fibronectin intensities for sprouts (following cells) or mini-sprouts are indicated as squares. (H) Fibronectin intensity of leading cells and following cells of sprouts, mini-sprouts, and quiescent cells. (I) Cellular layer was segmented into groups containing 7 neighboring cells to assess the local environment for each group. (J) Distributions of the ratio of cells having fibronectin levels higher than a threshold, the minimum value of sprout in (H), in a group of 7 neighboring cells defined in (I), which included either a sprout or a mini-sprout. The overall distribution covers both regions.



mini-sprouts (**Figs. 61 &J** ). The overall expression levels when all region types were combined was relatively uniform (**Fig. 6J** , third panel. Strikingly however, regions around sprouts (**Fig. 6J** , first panel) showed oppositely skewed patterns vs. mini-sprouts (**Fig. 6J** , second panel). Specifically, the fibronectin expression levels around sprouts were higher than the threshold, whereas the fibronectin levels around mini-sprouts were lower than the threshold. Altogether, these results supported the model in which fibronectin can indeed serve as a mediator of Turing-like induction of sprouting patterns, through re-modeling that enriches it at the points of sprout induction and depletes it at the points where Tip cells (mini-sprouts) are not stabilized to form full-fledged, lumenized sprouting bodies.

#### **Discussion**

A major challenge of the analysis of tissue development and homeostasis is understanding of how differentiation into distinct cell types can be robustly achieved, while also being sensitive to various pro-differentiation and morphogenic cues and, potentially affected by molecular noise in biochemical reactions. In the context of angiogenesis, this challenge more specifically relates to enabling effective vascular morphogenesis through robust yet environmentally responsive differentiation of endothelial cells into Tip and Stalk cells states. This process is guided by the mulTiple pro-angiogenic cues, such as VEGF and by the local tissue organization and mediated by the paracrine Delta-NOTCH cell signaling. Recent mathematical models of this process(28 , 29 ) have considered the robustness of the Delta-NOTCH differentiation to molecular noise, concluding that noisy biochemical reactions can both disrupt and enhance the spatial differentiation patterns, depending on the magnitude and spatial distribution (28 ). The effect of pro-angiogenic cues, such as VEGF on robustness of spatial differentiation patterning remains substantially less explored. Furthermore, compiling between modeling predictions and experimental validation has been challenged by the complexity of *in vivo* angiogenesis analysis, both on cellular and molecular levels.

Here, we integrated engineered experimental angiogenic assay and a spatially resolved computational modeling analysis to explore the spatially and temporally resolved effects of VEGF on angiogenic cell specification. Our results suggest that VEGF can have a dual role in inducing the initial Tip-Stalk cell differentiation. On the one hand, a low level of exogenous VEGF is essential to induce Delta-NOTCH signaling and the classical ordered 'salt-and-pepper' pattern, with approximately 25% of the cells adopting the Tip cell fate, as expected (30 ). This role of VEGF is conceptually similar to the classical case of EGF induced NOTCH signaling in C. elegans vulva development (31 2, 32 2). On the other hand, our results also suggest that an increase of VEGF levels can introduce disorder into this pattern, similar to order-disorder transition for various composite materials (12 2, 13 2), which may occur with increasing temperature and have the properties of a sharp phase transition. More specifically, high VEGF levels may play the role similar to an increased temperature in order-disorder transitions, leading to emergence of partially disordered 'salt-and-pepper 'structures. These disordered structures are characterized by higher than expected fractions of Tip cells and, consequently, an increased occurrences of otherwise disallowed adjacent Tip cells. Importantly, for all VEGF input levels and the resulting spatial patterns, the Tip-Stalk cell specification continued to be robust, although the degree of induction of NOTCH signaling was dependent on the VEGF dose. These results suggested that cell specification patterns deviating from the expected 'salt-and-pepper' one can develop not only due to noisy NOTCH signaling, as suggested by prior models, but also due to the control of the fractions of alternative cell states by the magnitude the pro-differentiation cue.

In spite of the observation that disordered 'salt-and-pepper' patterns still display robust differentiation, the spatial patterns of cell co-localization can generate inherent instabilities, e.g., due to two adjacent Tips mutually suppressing their fate selection through NOTCH signaling. Instabilities of this sort may increase the sensitivity of the differentiation process to additional



cues and can also lead to facilitated dynamic switching of cell fates (e.g., Tip to Stalk and vice versa) over prolonged periods of time. Such instabilities might lead to oscillatory-like fluctuations of NOTCH signaling as observed in other differentiation processes (33 2-35 2) and in endothelial cell sheets under high VEGF concentration inputs(36 2). Importantly, these instabilities may also underlie the striking observation of the continuous retraction and extension of mini-sprouts (protruding Tip cells) observed in our study. This dynamic fate-switching behavior can thus represent a signature of an unstable differentiation process that may either stabilize, in response to additional cues, leading to a specific morphogenetic outcome, such as the extension of a stable sprout, or display a prolonged instability resulting in a lack of pronounced morphogenesis. Such poised but unstable states may be similar to the undifferentiated state of neurogenic progenitors displaying oscillatory NOTCH signaling, which can proceed to differentiation after the oscillation is resolved into a temporally stable NOTCH activity (37 2).

The cues stabilizing cellular differentiation and morphogenesis can vary and represent the signature of both global and local pro- and anti-angiogenic environments. For instance, our prior analysis indicated that exposure of model parental vessels to VEGF only rather than a more complete pro-angiogenic cocktail of various factors, can result in formation of mini-sprouts (and hence, effective Tip-Stalk cell differentiation), but not full-fledged sprouts (7 ). Sprout formation may also be modulated by the presence of mural cells and pro-inflammatory cytokines, which can indirectly modulate the NOTCH activity, but could also have additional effects, serving to stabilize a specific differentiation outcome. However, even if sprouts do form, it is not clear how their spatial distribution may arise and be potentially controlled by the environmental inputs. Our results argue that, for a given number of sprouts forming in the parental vessel, their mutual distances are maximized. This spatial distribution is consistent with a Turing-like mechanism (19 🖒 , 20 🖒 ), implying the existence of a long-distance interaction inhibiting formation of new sprouts in the vicinity of the existing ones. Although the actual mechanism of putative Turninglike pattern formation is not fully elucidated here, our results are consistent with a variant of this regulatory behavior, in which a component of the extracellular matrix, fibronectin is actively redistributed by the nascent sprouts, with this ECM component being enriched at the points of sprout formation, but depleted in other zones, thus preventing sprout induction in the depleted areas. This redistribution is indeed equivalent to the classical Turing mechanisms that would involve generation of an explicitly inhibitory compound by the growing sprouts. Fibronectin has been implicated as a key pro-angiogenic ECM component, possibly due to its integration with VEGF, which further increases the plausibility of this mechanism (25 ♂). Interestingly, we find elevated levels of fibronectin at the bases of extending sprouts, but not at their Tips. This finding has two implications. First, fibronectin may be an important factor in the sprout induction rather than extension, hence the growing sprout can progress into the surrounding matrix beyond the area of enriched fibronectin, leaving it behind. Secondly, fibronectin can also promote lumen formation (26 🖒, 27 🖒), thus its enrichment at the bases of extending sprouts can further contribute to their lumenized structure. Furthermore, this mechanism can help explain the dramatic influence of cytokines, such as TNF, in preventing sprout formation, which can happen in sharp, TNF dose-dependent manner (7 ). Indeed, TNF avidly binds to fibronectin (24 ) and therefore, at high enough concentrations, would have a particular anti-angiogenic effect in the areas of increased fibronectin density, which according to the proposed mechanism would be the areas of incipient sprouts. This would dramatically increase its anti-sprouting effect, even if the effect of this cytokine on the NOTCH-dependent cell specification is more muted (7 🖒). Of note, another version of the Turing mechanism has recently been suggested to account for the branching of the sprouts, also involving formation of new Tip cells leading individual branches, although the molecular mechanism postulated in that analysis was distinct from the one proposed here (38 2, 39 2). These models, though plausible, will need to be further tested to ascertain causality of the proposed mechanisms, although at this stage the Turing-like mechanisms appear to be the best candidates to explain the experimental results we obtained.



Overall, our analysis supports the following dynamic view of angiogenic induction. The VEGF input can induce NOTCH signaling and formation of Tip cells that can behave as mini-sprouts. At lower VEGF input, a more ordered pattern of Tip cell induction can lead to formation of approximately 25% of Tip cells, but relatively few of these will become sprouts, reflecting lower sensitivity to additional ambient cues, promoting sprout formation. On the other hand, at higher VEGF inputs, a greater disorder of Tip cell patterning permits higher sensitivity to external cues, such as fibronectin, that can stabilize the sprouting. In addition, a more frequent co-localization of Tip cells under this condition enables initiation of a sprout from two adjacent cells, as observed in a fraction of cases in our experiments (the case in **Table 1** involving formation of a sprout by two adjacent cells). The initial emergence of sprouts leads to a progressively less likely sprout formation and to the overall maximization of the distance between the sprouts. Both these observations are consistent with non-local inhibition of sprout formation around the sprouts that have already formed. A plausible mechanism for this inhibition and the overall pattern formation is the re-distribution of fibronectin from the zones between sprouts towards the incipient sprouts, constituting both a positive and negative feedback loops, commonly assumed in a variant of the Turing patterns from action. This mechanism is very sensitive to various local inputs distinct from VEGF and fibronectin, which can further influence the location and density of the developing blood vessels. These may include the effects of pericytes or local inflammatory environments, as mentioned above, but also other ECM components, such as collagens, that may enhance the protrusion of Tip cells and thus stabilize the emergent sprouts both directly and indirectly. Endothelial fate induction process may be interesting to contrast with other complex multicellular processes, including collective epithelial migration, where NOTCH signaling similarly modulates fine-grained patterns of leader and follower cells (40 🖒), and underscore the need in the future to develop more refined models that explicitly integrate the interconnections between biochemical and mechanical regulation of Tip-Stalk fate(41 22). The results in this study can further inform our understanding of angiogenesis in physiological and patho-physiological conditions. In particular, in many circumstances, the levels of VEGF is determined by the degree of hypoxia, which can be highly elevated following oxygen supply interruption, e.g., in wound healing or ischemia, or due to progression of neoplastic growth. Our results suggest that in these cases, formation of sprouts can be dysregulated due to higher incidences of co-localizations of prospective Tip cells. In addition, since these conditions are frequently accompanied by altered synthesis of ECM, the sprout density can increase, which may lead to formation of denser and less developed vascular beds frequently observed as a result of tumor angiogenesis(42 🖒, 43 🖒). Our results thus suggest that the disorder and higher plasticity of the endothelial cell fate speciation at higher VEGF inputs can be a key contributor to some pathological states associated with persistently hypoxic conditions.

The analysis presented here highlights the utility of combining experimental engineered vasculature models with mathematical analysis as integrated research platforms to gain a progressively better insight into angiogenesis in highly controlled micro-environments. Although, questions remain about the mechanistic underpinnings of the phenomena observed here and in related studies, the analysis enabled by these model systems can help formulate guiding hypotheses for further understanding of angiogenesis *in vivo*, while decoupling the complexities of the native angiogenic environments. We anticipate that the dynamic exploration presented here can help pave the way for further quantitative understanding of this key biological process.

#### **Materials and Methods**

Chips for mimicking 3D angiogenesis *in vitro* were fabricated as introduced in our previous work(7 ). Fluorescence images of the *in vitro* model were acquired by Lecia scanning disk confocal microscopy, and the z-stack images were processed with IMARIS (Bitplane) to quantify Tip-Tip distance, to track the positions of sprouts and mini-sprouts, and to analyze fibronectin intensity distribution. We generalized existing mathematical models of the interconnected signaling between the NOTCH and VEGF pathways to a two-dimensional multicellular scenario



#### **Acknowledgements**

This work was supported by NIH through NCI U54 CA209992 (to A.L.); Mia Neri Foundation (to T.-Y.K.); The Center for Theoretical Biological Physics sponsored by the NSF (Grant PHY-2019745), NSF-PHY-2210291, CPRIT Scholar in Cancer Research sponsored by the Cancer Prevention and Research Institute of Texas (to J.N.O.); a Simons Foundation grant 594598 (to Q.N.). F.B. was supported by a National Science Foundation grant DMS1763272 (Q.N.).

Parameter type	Parameter	Value	Units
Production	$N_0, D_0, J_0, V_{R0}$	1200,1000,800, 1000	Molecule/hour
Degradation	$\gamma, \gamma_I$	0.1, 0.5	1/hour
Binding	$k_T, k_C$	2.5 10 <sup>-5</sup> , 5 10 <sup>-4</sup>	1/(molecule hour)
Hill threshold	$I_0, V_0$	200, 80*	Molecules
Fold-change	$\lambda_N, \lambda_{I,D}, \lambda_{V,I}, \lambda_J, \lambda_V$	2, 0, 0, 2, 2	Dimensionless
Hill coefficient	$n_N, n_{I,D}, n_{V,I}, n_J, n_V$	2, 2, 2, 5, 2	Dimensionless

#### Table 2.

Parameter values for simulation. \*Rescaled from previous model to match experimental observation.



#### References

- 1. Adams R. H., Alitalo K. (2007) **Molecular regulation of angiogenesis and lymphangiogenesis** *Nat Rev Mol Cell Biol* **8**:464–478
- Potente M., Gerhardt H., Carmeliet P. (2011) Basic and therapeutic aspects of angiogenesis Cell 146:873–887
- 3. Benedito R., et al. (2009) **The NOTCH ligands Dll4 and Jagged1 have opposing effects on angiogenesis** *Cell* **137**:1124–1135
- 4. Blanco R., Gerhardt H. (2013) **VEGF and NOTCH in Tip and Stalk cell selection** *Cold Spring Harb Perspect Med* **3**
- 5. Wang W. Y., Lin D., Jarman E. H., Polacheck W. J., Baker B. M. (2020) **Functional angiogenesis** requires microenvironmental cues balancing endothelial cell migration and proliferation *Lab Chip* **20**:1153–1166
- 6. Liu J., et al. (2021) Synthetic extracellular matrices with tailored adhesiveness and degradability support lumen formation during angiogenic sprouting *Nat Commun* 12
- 7. Kang T. Y., et al. (2019) **Pericytes enable effective angiogenesis in the presence of proinflammatory signals** *Proc Natl Acad Sci U S A* **116**:23551–23561
- 8. Chen M. B., et al. (2017) **On-chip human microvasculature assay for visualization and quantification of tumor cell extravasation dynamics** *Nat Protoc* **12**:865–880
- 9. Nguyen D. H., et al. (2013) **Biomimetic model to reconstitute angiogenic sprouting** morphogenesis in vitro *Proc Natl Acad Sci U S A* **110**:6712–6717
- 10. Boareto M., et al. (2015) **Jagged-Delta asymmetry in NOTCH signaling can give rise to a Sender/Receiver hybrid phenotype** *Proc Natl Acad Sci U S A* **112**:E402–409
- 11. Bocci F., Onuchic J. N., Jolly M. K. (2020) **Understanding the Principles of Pattern Formation Driven by NOTCH Signaling by Integrating Experiments and Theoretical Models** *Front Physiol* **11**
- 12. Yang Y., et al. (2017) **Deciphering chemical order/disorder and material properties at the single-atom level** *Nature* **542**:75–79
- 13. Bu K., et al. (2022) **Nested order-disorder framework containing a crystalline matrix with self-filled amorphous-like innards** *Nat Commun* **13**
- 14. Shaya O., et al. (2017) **Cell-Cell Contact Area Affects NOTCH Signaling and NOTCH- Dependent Patterning** *Dev Cell* **40**:505–511
- 15. Kwak M., et al. (2022) Adherens junctions organize size-selective proteolytic hotspots critical for NOTCH signalling *Nat Cell Biol* **24**:1739–1753
- Liu D. L., An M., Johnson I. R., Lovett J. V. (2003) Mathematical Modeling of Allelopathy. III. A Model for Curve-Fitting Allelochemical Dose Responses Nonlinearity Biol Toxicol Med 1:37–50



- 17. Fraenkel G. S. (1959) The raison d'etre of secondary plant substances; these odd chemicals arose as a means of protecting plants from insects and now guide insects to food *Science* 129:1466–1470
- 18. Willis R. J. (2007) The history of allelopathy
- 19. Turing A. M. (1990) The chemical basis of morphogenesis. 1953 Bull Math Biol 52:153–197
- 20. Maini P. K., Baker R. E., Chuong C. M. (2006) **Developmental biology. The Turing model comes of molecular age** *Science* **314**:1397–1398
- 21. Feng X., Tonnesen M. G., Mousa S. A., Clark R. A. (2013) **Fibrin and collagen differentially but** synergistically regulate sprout angiogenesis of human dermal microvascular endothelial cells in 3-dimensional matrix *Int | Cell Biol* **2013**
- 22. Senk A., Djonov V. (2021) **Collagen fibers provide guidance cues for capillary regrowth** during regenerative angiogenesis in zebrafish *Sci Rep* 11
- 23. Kirkpatrick N. D., Andreou S., Hoying J. B., Utzinger U. (2007) **Live imaging of collagen remodeling during angiogenesis** *Am J Physiol Heart Circ Physiol* **292**:H3198–3206
- 24. Alon R., et al. (1994) **TNF-alpha binds to the N-terminal domain of fibronectin and augments the beta 1-integrin-mediated adhesion of CD4+ T lymphocytes to the glycoprotein** *J Immunol* **152**:1304–1313
- 25. Wijelath E. S., et al. (2006) **Heparin-II domain of fibronectin is a vascular endothelial** growth factor-binding domain: enhancement of VEGF biological activity by a singular growth factor/matrix protein synergism *Circ Res* 99:853–860
- 26. Astrof S., Hynes R. O. (2009) **Fibronectins in vascular morphogenesis** *Angiogenesis* **12**:165–175
- 27. Bayless K. J., Salazar R., Davis G. E. (2000) **RGD-dependent vacuolation and lumen formation observed during endothelial cell morphogenesis in three-dimensional fibrin matrices involves the alpha(v)beta(3) and alpha(5)beta(1) integrins** *Am J Pathol* **156**:1673–1683
- 28. Galbraith M., Bocci F., Onuchic J. N. (2022) **Stochastic fluctuations promote ordered pattern formation of cells in the NOTCH-Delta signaling pathway** *PLoS Comput Biol* **18**
- 29. Koon Y. L., Zhang S., Rahmat M. B., Koh C. G., Chiam K. H. (2018) Enhanced Delta-NOTCH
  Lateral Inhibition Model Incorporating Intracellular NOTCH Heterogeneity and TensionDependent Rate of Delta-NOTCH Binding that Reproduces Sprouting Angiogenesis
  Patterns Sci Rep 8
- 30. Collier J. R., Monk N. A., Maini P. K., Lewis J. H. (1996) **Pattern formation by lateral inhibition** with feedback: a mathematical model of delta-NOTCH intercellular signalling *J Theor Biol* **183**:429–446
- 31. Shin H., Reiner D. J. (2018) **The Signaling Network Controlling C. elegans Vulval Cell Fate**Patterning *J Dev Biol* **6**
- 32. Yoo A. S., Bais C., Greenwald I. (2004) **CrosStalk between the EGFR and LIN-12/NOTCH** pathways in C. elegans vulval development *Science* 303:663–666



- 33. Zhang Y., et al. (2021) **Oscillations of Delta-like1 regulate the balance between differentiation and maintenance of muscle stem cells** *Nat Commun* **12**
- 34. Venzin O. F., Oates A. C. (2020) What are you synching about? Emerging complexity of NOTCH signaling in the segmentation clock *Dev Biol* 460:40–54
- 35. Kageyama R., Niwa Y., Shimojo H., Kobayashi T., Ohtsuka T. (2010) **Ultradian oscillations in NOTCH signaling regulate dynamic biological events** *Curr Top Dev Biol* **92**:311–331
- 36. Ubezio B., et al. (2016) Synchronization of endothelial Dll4-NOTCH dynamics switch blood vessels from branching to expansion *Elife* 5
- 37. Shimojo H., Ohtsuka T., Kageyama R. (2008) **Oscillations in NOTCH signaling regulate** maintenance of neural progenitors *Neuron* **58**:52–64
- 38. Guo S., Sun M. Z., Zhao X. (2021) **Wavelength of a Turing-type mechanism regulates the morphogenesis of meshwork patterns** *Sci Rep* **11**
- 39. Xu H., Sun M., Zhao X. (2017) **Turing mechanism underlying a branching model for lung morphogenesis** *PLoS One* **12**
- 40. Mercedes S. A. Vilchez, et al. (2021) **Decoding leader cells in collective cancer invasion** *Nat Rev Cancer* **21**:592–604
- 41. Stassen O., Ristori T., Sahlgren C. M. (2020) **NOTCH in mechanotransduction from** molecular mechanosensitivity to tissue mechanostasis / *Cell Sci* 133
- 42. Ruoslahti E. (2002) **Specialization of tumour vasculature** *Nat Rev Cancer* **2**:83–90
- 43. Chung A. S., Lee J., Ferrara N. (2010) **Targeting the tumour vasculature: insights from physiological angiogenesis** *Nat Rev Cancer* **10**:505–514
- 44. Boareto M., Jolly M. K., Ben-Jacob E., Onuchic J. N. (2015) **Jagged mediates differences in normal and tumor angiogenesis by affecting Tip-Stalk fate decision** *Proc Natl Acad Sci U S A* **112**:E3836–3844

#### Article and author information

#### Tae-Yun Kang

Department of Biomedical Engineering, Yale University ORCID iD: 0000-0002-6122-0870

#### **Federico Bocci**

NSF-Simons Center for Multiscale Cell Fate Research, University of California Irvine, Department of Mathematics, University of California Irvine ORCID iD: 0000-0003-4302-9906

#### **Qing Nie**

NSF-Simons Center for Multiscale Cell Fate Research, University of California Irvine, Department of Mathematics, University of California Irvine ORCID iD: 0000-0002-8804-3368



#### José Nelson Onuchic

Center for Theoretical Biological Physics, Rice University For correspondence: jonuchic@rice.edu

ORCID iD: 0000-0002-9448-0388

#### **Andre Levchenko**

Department of Biomedical Engineering, Yale University For correspondence: andre.levchenko@yale.edu

ORCID iD: 0000-0001-6262-1222

#### Copyright

© 2023, Kang et al.

This article is distributed under the terms of the Creative Commons Attribution License, which permits unrestricted use and redistribution provided that the original author and source are credited.

#### **Editors**

Reviewing Editor

**Daniel Henrion** 

University of Angers, Angers, France

Senior Editor

#### **Matthias Barton**

University of Zurich, Zurich, Switzerland

#### Reviewer #1 (Public Review):

The authors succeeded in establishing experimental and mathematical models for the formation of new blood vessels. The experimental model relies on temporal imaging of multilcellular projections and lumen formation from a single blood vessel embedded in an engineered extracellular matrix. The mathematical model combines both discrete and continuum elements. It would be helpful to understand how the authors came up with phenotypic classes for analyzing their live imaging data. On the modeling side, it would be useful to see whether the claims about Turing patterns could be supported by either a meanfield model or a more thorough parametric analysis of the discreet continuum model. The authors did a good job in comparing their VEGF/Notch mechanism to the EGF/Notch vulval patterning mechanism in C. elegans. The authors might want to look into the literature from studies of the tracheal patterning system in Drosophila when the combined actions of the FGF and Notch signaling specify tip and stalk cells. The similarities are quite striking and are worth noting.

https://doi.org/10.7554/eLife.89262.2.sa1

#### Reviewer #2 (Public Review):

#### Summary:

In this manuscript, the goal of the authors is to understand the process of mature sprout formation from mini-sprouts to develop new blood vessels during angiogenesis. For this, they use their earlier experimental setup of engineered blood vessels in combination with a



modified spatio-temporal model for Notch signalling. The authors first study the role of VEGF on Tip (Delta-rich) and Stalk (Notch-rich) patterning. The Tip cells are further examined for their space-time dynamics as Mini-sprouts and mature Sprouts. The Notch signalling model is later supplemented with a phenomenological \_random uniform model\_ for Sprout selection as a plausible mechanism for Sprout formation from Mini-Sprouts. Finally, the authors look into the role of fibronectin in the Sprout formation process. Overall, the authors propose that VEGF interacts with Notch signalling in blood vessels to generate spatially disordered and colocalized Tip cells. VEGF and fibronectin then provide external cues to dynamically modulate mature Sprout formation from Mini-Sprouts that could control the location and density of developing blood vessels with a process that is consistent with a Turing-like mechanism.

#### Strengths and Weaknesses

In this manuscript, work motivation, problem definition, experimental procedures, analysis techniques, mathematical methods (including the parameters), and findings are all presented quite clearly. Moreover, the authors carefully indicate whenever they make any assumptions, and do not mix unproven hypothesis with deduced or known facts. The experimental techniques and most of the mathematical methods used in this paper are borrowed from the earlier works of the corresponding authors, and thus are not completely novel. However, the use of these ideas to provide a simple elucidation of the role of VEGF and fibronectin in Sprout formation, in an otherwise complex system, is very interesting and useful. Some of the data analysis methods presented in the paper - (i) quantification of Tip spatial patterns (Fig. 3) and (ii) Sprout temporal dynamics using Sankey diagram (Fig. 4) - seem quite novel to me in the context of Notch signalling literature. Similarly, the authors also provide a new mechanism (VEGF) to obtain disordered Delta-Notch patterning without explicitly including \_noise\_ in the system (Fig. 2 and Fig. S1). The authors also systematically quantify the statistics of spacing between the Sprouts and show that the Sprouts have a tendency to be away from each other, something that they could also partially recapitulate by additionally including a novel \_random uniform model\_ for Sprout selection (Fig. 5). Although the association between fibronectin and angiogenesis is known in the literature, in this manuscript, the authors could clearly demonstrate that fibronectin is present in high and low levels, respectively, around Sprouts and Mini-sprouts (Fig. 6). A combination of these findings could then motivate the authors to hypothesize, as mentioned above, a Turing-like mechanism for Sprout formation, something that I find interesting.

Although I find the relative simplicity of the experimental system and theoretical model and the clear findings they generate appealing, some aspects raise a few questions. The authors experimentally find 20 +- 0.08 percent of Tip cells in the model blood-vessels that is consistent with the salt-and-pepper pattern seen in Notch signalling model (~25 %). However, it is not clear to me if the reverse is true, i.e., 25% of Tip cells automatically imply a salt-and-pepper pattern - the authors do not seem to provide a direct experimental evidence. Furthermore, the authors use their Notch signalling model on a regular hexagonal lattice, but there is a large variability in the cell sizes (Fig. 3) in the experimental system. Since it is observed in the literature that signalling depends on the contact area between the neighbouring cells, it is not clear how that would affect the findings presented in this paper. Similarly, since some of the cells are quite small compared to the others, I worry how appropriate it is to express the distance between the Tip cells in terms of \_cell numbers\_ (Fig. 3). Regarding Sprout classification, as per Table 1, a bridge of two cells is formed as per early-stage-I mechanism for Sprout. On the other hand, the entire data interpretation of experiments seems to be based on early Stage II and matured stage in that same table (also Figs. 3 and 4) in which only one Tip cell seems to be counted per mature Sprout. However, if some Sprouts are formed via early stage-I mechanism, a projection in 2D for analysis would give a count of two adjacent Tip cells, but corresponding to a \_single\_ Sprout. It could be possible that the presence of such two-cell Sprouts affects the statistics of inter-Sprout distances (Fig. 5). Finally, I find the proposed mechanism of Sprout formation dynamics to be somewhat



unsatisfactory. Other than the experimental evidence regarding the spacing of Sprouts and the fibronectin levels around Sprouts and Mini-sprouts (Figs. 4 and 5), there is very little evidence to support the hypothesis about a Turing-like mechanism for Sprouting. Moreover, it seems to me that Turing patterns can appear in a wide variety of settings and could be applied to the current problem in an abstract manner without making any meaningful connections with the system variables. Also, from a modeling point of view, cell migration and mechanics, are expected to take a major part in Sprout formation, while cell division and inclusion would most likely influence Tip-Stalk cell formation. However, it seems that in the present work, these effects are coarse-grained into Notch signalling parameters and the Sprout selection model, thus making any experimental connection quite vague.

#### Overall Assessment

I feel that the authors, on the whole, do achieve their main goals. Although I have a few concerns that I have raised above, overall, I find the work presented in this manuscript to be a solid addition to the broad field of collective cell dynamics. The authors use well established experimental and mathematical methods while adding a few novel analysis techniques and modeling ideas to provide a compelling, albeit incomplete, picture of Sprout formation during angiogenesis. While the direct application of this work in the context of angiogenesis is obvious, the broad set of ideas and techniques (discussed above) in this work would also be useful to researchers who work on Notch signalling in morphogenesis, collective cell migration, and epithelial-mesenchymal-transition.

https://doi.org/10.7554/eLife.89262.2.sa0

#### **Author Response**

The following is the authors' response to the original reviews.

#### Reviewer #1 (Recommendations For The Authors):

1. A more thorough analysis of transition boundaries between different types of patterns would further strengthen the conclusions.

We agree that the transition between different patterning regimes should be discussed more quantitatively in the manuscript. Specifically, we identified a highly sensitive parameter range where the disorder in the patterns rapidly increases as a function of the VEGF stimulus. We have improved our discussion of the transition between 'orderedlike' patterns and 'disordered-like' patterns in the main text as follows: "At relatively low VEGF levels, the patterns were mostly ordered, with small deviations from the expected 'salt and paper' geometry with a 25%-75% ratio of TipStalk (Fig. 2D). However, as the VEGF input increased, the fraction of Tips grew and the patterns became sharply more disordered over a relatively narrow range of magnitude of the VEGF input, which could be identified as a highly sensitive area separating more 'ordered-like' and 'disordered-like' patterns. Finally, increasing VEGF stimuli beyond the highly sensitive area further increased the disorder of the patterns, but with a lower VEGF sensitivity, over several more orders of magnitude of VEGF inputs".

#### Reviewer #2 (Recommendations For The Authors):

Please refer to the Public Comments above for a broad review. Below, I provide specific concerns that could be addressed.

Main comments



Is the salt-and-pepper model observed for the case when there is no VEGF in the
experiments? It would be good to confirm the same. If not, the analysis presented in Fig.
3 could be performed for this case and used as a baseline while referring to the data in
Fig. 3.

We thank the referee for the interesting suggestion. The pattern predicted by the model is not strictly salt-and-pepper in absence of VEGF, but the disorder quantified in terms of "incorrect" contacts between Tip cells is considerably lower (see for example the disorder quantification in supplementary figure 1C). We have included the Tip-Tip contact statistics for a case of VEGF=1 ng/ml (100-fold lower that the level used in Fig. 3 compare between model and experiment). In this case, there is clearly more spacing between Tip cells, thus demonstrating how high VEGF stimuli increase the probability of contacts between Tip cells. In the main text, we commented: "As a baseline comparison, the mathematical model with a 100-fold reduction of VEGF stimulus (1 ng/ml) exhibited a Tip-Tip distance statistics more closely comparable with the 'salt-and-pepper' model".

1. The authors mention in the Discussion (end of pg. 7) that ...a low level of exogeneous VEGF is essential to induce Delta-NOTCH signalling.. However, in the standard NOTCH signalling (Boareto et al.), we can get the salt-and-pepper pattern without any VEGF. Am I missing something? The authors may want to take a re-look.

We appreciate the referee's understanding of the mathematical model. The model used here still exhibits a bistable behavior between the low-Delta and high-Delta cell states even in the absence of VEGF input, as seen for example in the cell state distribution of Fig. 2B, and in agreement with the original model by Boareto et al. This behavior is reflective of the more general applicability of the model, as it describes Delta-NOTCH interactions in various systems. For endothelial cells, VEGF is indeed required to trigger this interaction, but this was not the primary focus of the paper, hence the original model was used. In the text referred to by the reviewer, we are discussing the role, of VEGF based in its known biological effects as well as modeling results. We anticipate that the future further adaptation of the model to, endothelial cells will refine its description of of cell interactions in the absence of VEGF.

1. The size of cells (or spacing between cell nuclei) is highly variable (Fig. 3). Since it is known that the size of cell-cell junctions influences signalling, it would good to at least comment on the same, considering that the model in the paper consists of regular static hexagons. Similarly, it seems desirable to comment on expressing the distance between Tip cells (Fig. 3) in cell length units, when the cell lengths are so variable.

We concur with the suggestion that our consideration of the cell-cell contact size in NOTCH signaling should be clarified in the manuscript.

Sprinzak et al. reported in their 2017 article published in Developmental Cell that the cell-cell contact area does influence NOTCH Signaling. In this article, they found that NOTCH transendocytosis (TEC) for pairs with a larger contact width (25 $\mu$ m) is up to five times higher than for pairs with a smaller contact (2.5 $\mu$ m), as observed through the two-cell TEC assay. While TEC correlates with contact width across a range from 1 to 40 $\mu$ m, the values fluctuate significantly in the middle range, particularly when excluding extremely low cell-cell contact areas.

In our experiments, we observed that the cell-cell contact area ranges from essentially infinitesimal corner-to-corner contact to roughly 50µm. We excluded the corner contacts,



which might correspond to extremely low cell-cell contact areas, from the Tip-Tip distance measurements as depicted in Fig. 3B. We also made the assumption that variations in cell-cell contact size within tens of microns correlate weakly with the strength of NOTCH signaling. This assumption did not impede our effort to compare the overall trends with results from modeling using hexagonal cells, as shown in Figs 6 D&E. We have included this comment and the corresponding reference to elucidate our assumption in the results as follows: In our experiments, the observed cell-cell contact area varied, spanning from very low (cell cornerto-corner contact) up to approximately 50µm. Previous studies(14, 15) have clearly demonstrated the influence of the cell-cell contact area on NOTCH Signaling, but the values get nosy in the middle range, particularly when excluding extremely low cell-cell contact areas. Reflecting these findings, we excluded the corner contacts, which might correspond to extremely low cell-cell contact areas, from the Tip-Tip distance measurements as depicted in Fig. 3B. We also made an assumption that variations in cell-cell contact size within tens of microns correlate weakly with the strength of NOTCH signaling. This assumption did not impede our effort to compare the overall trends with results from modeling using hexagonal cells, as shown in Figs 3 D&E.

1. The results presented in Fig. 6J are quite striking. However, the number of samples N = 10 and N = 11 seem somewhat low. How does one justify that the findings are not influenced by low number fluctuations?

We acknowledge the reviewer's concerns regarding potential biases stemming from a limited number of samples. The analysis presented in Fig. 6J was specifically designed to complement and support the findings in Fig. 6H. In this context, the counts of sprout and mini-sprout dots correspond to the number of instances "including a sprout" and "including a mini-sprout."

While the counts of sprouts and mini-sprouts in Fig. 6H might seem limited as highlighted by the reviewer, the statistical difference between the two groups was found to be significant. Nevertheless, we expanded our regions of interest to encompass neighboring cells, based on the rationale that the local environment might have closely interacting and similar features. The sample sizes in Figure 6J, represented as N=10 and N=11, equate to an examination of 70 cells and 77 cells, respectively. For instance, in the category "including a sprout," five out of ten groups indicated that all seven neighboring cells in a group exhibited fibronectin levels exceeding a given threshold, translating to 35 cells with fibronectin levels above this threshold. Given that the observed trends in distribution were consistently reasonable across the examinations of both 70 and 77 cells, we would like to state that we are confident in our results.

1. It is written towards the end on pg. 5 that ... although all sprouts indeed formed from mini-sprouts, not all .... However, as can be seen from Fig. 40, Sprouts can also be generated from Stalk cells. This should be corrected.

Thank you for highlighting the discrepancy between our statement on page 5 and the observations in Fig. 40. While all sprouts undergo a mini-sprout phase, the transition from Stalk to mini-sprout is not always be observed due to the limitations of our observational timeframe. We acknowledge this oversight and adjusted our statement to clarify that sprouts appearing to form directly from Stalks likely passed through an unobserved intermediate mini-sprout stage as follows: We found that all sprouts formed either directly from Stalks or from mini-sprouts, suggesting a non-observed transition from Stalk to mini-sprout due to observational timeframe limitations. Strikingly, however, not all minisprouts persisted and initiated sprout formation.

1. No solid blue bars are shown in Fig. S2A as mentioned in the caption. Kindly correct.



We apologize for the mistake. We have corrected the figure to show the blue bars depicting the experimental measurements for sprout distance probability.

1. How are the high-Delta cells or high-NOTCH cells decided in experiments or simulations? Does it happen that Delta and NOTCH levels are comparable? In that case, what is done? This point could be clarified in the main manuscript or Materials and Methods.

We agree with the reviewer that Tip cell definition should be clarified. In the model, we define a threshold level for cellular Delta to distinguish Tip and Stalk cells, which is now explained in the Methods section "Definition of Tip cells in the model". As elaborated in the new section, Delta and NOTCH levels are never comparable due to the circuit's bistable behavior. In experiments, Tip cells based on their key phenotypic characteristic — invasive migration into the surrounding collagen matrix rather than Delta or NOTCH levels. The details can be found in "Precise quantification of Tip cell spatial arrangement suggests disordered patterning in the engineered angiogenesis model" section and Figure 3A.

#### Minor comments

There are a good number of typos in the paper. The manuscript should be carefully checked and corrected for the same. Below, I provide a few instances.

- 1. In the abstract towards the end, it should be "understanding" instead of "understating"
- 1. On pg. 5, just before the beginning of the last paragraph, there is a typo "parodied" which should most likely be "provided"
- 1. First paragraph on pg. 6 typo "spouts" instead of "Sprouts"
- 1. Second paragraph on pg. 6, correctly write "testS"
- 1. Near the beginning of pg. 8, should be "C. elegans" instead of "C. elegance"
- 1. Figure 1 caption, towards the end, should be "Stalk" instead of "Salk"

We sincerely appreciate your keen attention to detail. we have thoroughly reviewed the manuscript and made the necessary corrections, including those that you have highlighted.

#### Reviewer #3 (Recommendations For The Authors):

Major concern:

The authors should discuss in more detail how their work can be used for a better understanding of the angiogenesis process in physiological conditions and in pathological conditions such as post-ischemic revascularization or tumor vascularization.

We have included comments and the corresponding references to clarify the aspect the reviewer suggested: The results in this study can further inform our understanding of angiogenesis in physiological and pathophysiological conditions. In particular, in many circumstances, the levels of VEGF is determined by the degree of hypoxia, which can be highly elevated following oxygen supply interruption, e.g., in wound healing or ischemia, or



due to progression of neoplastic growth. Our results suggest that in these cases, formation of sprouts can be dysregulated due to higher incidences of co-localizations of prospective Tip cells. In addition, since these conditions are frequently accompanied by altered synthesis of ECM, the sprout density can increase, which may lead to formation of denser and less developed vascular beds frequently observed as a result of tumor angiogenesis(42, 43). Our results thus suggest that the disorder and higher plasticity of the endothelial cell fate speciation at higher VEGF inputs can be a key contributor to some pathological states associated with persistently hypoxic conditions.